Single-Molecule Spectroscopy of Conjugated Polymers

PAUL F. BARBARA,* ANDRE J. GESQUIERE, SO-JUNG PARK, AND YOUNG JONG LEE

Center for Nano- and Molecular Science and Technology and Department of Chemistry and Biochemistry, University of Texas at Austin, Austin, Texas 78712

Received March 10, 2005

ABSTRACT

The molecular structure, photochemistry, and device physics of conjugated polymers have been investigated by single-molecule spectroscopy (SMS), using the unique ability of this technique to unravel complex spectra and dynamics. Surprisingly efficient and directional electronic energy funneling was observed for conjugated polymer molecules due to highly ordered conformations. Furthermore, recent studies on the SMS of conjugated polymers embedded in electronic devices demonstrate that SMS is a powerful tool for studying the photophysics and charge-transfer processes of conjugated polymers, giving new insights into the complex interactions among excited and charged species that exist in a device environment.

Introduction and Overview

Conjugated polymers are widely used as active materials (emitter, sensors, conductors, etc.) in a broad range of electronic devices including organic light emitting diodes (OLEDs) for flat panel displays, photovoltaic devices for solar energy conversion, thin-film transistors, and chemical sensors.[1−3] Figure 1A portrays a typical OLED device architecture and associated energy-level diagram. The device includes an indium tin oxide (ITO) anode where hole polarons (cations) are injected, a conjugated polymer hole transport layer, a different conjugated polymer layer where electron polarons are transported and electroluminescence is generated by electron/hole recombination, and finally a metal cathode, where electron polarons (anions) are injected. Unfortunately, it is extremely difficult to unravel the complex and heterogeneous kinetics in such a device. First, there are many different types of S_1 singlet excitons (excited states), T_1 triplet excitons, and

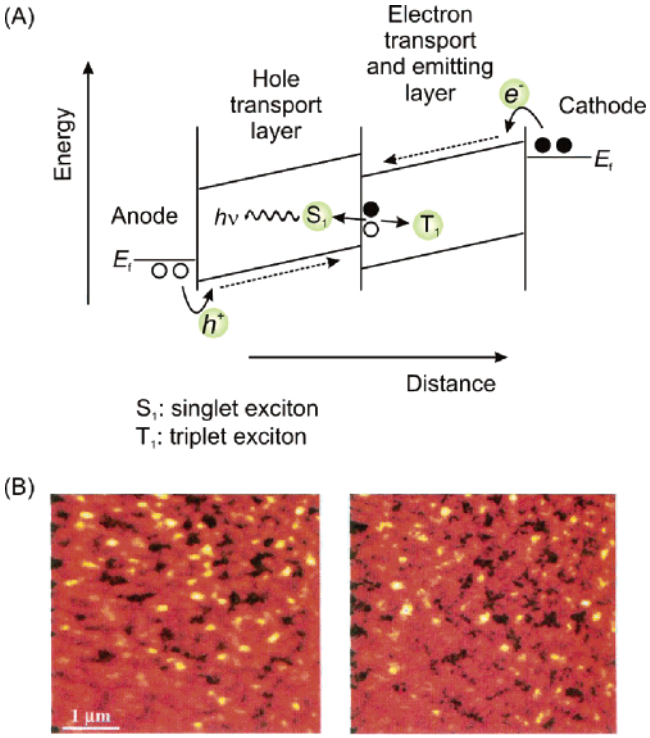

FIGURE 1. (A) A schematic band energy diagram for a two layer OLED and (B) near-field scanning optical microscopy (NSOM) images of a typical conjugated polymer thin film, see ref 4.

charged species (polarons) in a device, leading to large spatial variations and fluctuations in the kinetics of these species. Second, conjugated polymers have a complex nanostructure associated with morphological features (polymer chain folding, packing, and aggregation), which can seriously impact the operation of a device. The diverse nanoscale morphologies of conjugated polymers have been revealed, for example, in the polarization-sensitive near-field scanning optical microscopy images of these materials, as shown in Figure 1B.[4]

The complex chemical and physical processes of heterogeneous systems are often obscured in ordinary ensemble measurements. These processes, however, have become accessible in recent years through the application of single-molecule (single-particle) experimental tools,

Paul Barbara was born in New York, NY, in 1953. He attended Hofstra University, earning a B.A. in 1974, and then went on to perform graduate work with R. G. Lawler at Brown University, receiving his Ph.D. in Chemistry in 1978. From 1978 to 1980, he carried out postdoctoral work at Bell Laboratories. He joined the faculty of the University of Minnesota in 1980, achieving the rank of full professor in 1990. In 1995, he was named 3M-Alumni Distinguished Professor of Chemistry. In 1998, he moved to the University of Texas, Austin, to fill the Richard J. V. Johnson Welch Chair in Chemistry, which he holds presently along with the title Director of the Center for Nano- and Molecular Science and Technology. He is currently a Senior Editor of *Accounts of Chemical Research* and a Past Chair of the Division of Physical Chemistry of the American Chemical Society. He was elected to the American Academy of Arts and Sciences in 1999 and was elected Fellow of the American Physical Society in 1993 and Fellow of the American Association for Advancement of Science in 2004. His research interests include nanoscience, ultrafast chemical reaction dynamics in solution, radiation chemistry, photochemistry femtosecond spectroscopy, near-field scanning optical microscopy, and single-molecule spectroscopy. He has published over 190 articles and book chapters.

Andre J. Gesquiere obtained his Ph.D. in 2001 in the group of Frans De Schryver at K. U. Leuven, Belgium, where he worked on the characterization of organic supramolecular systems. After a postdoctoral stay in the group of E. W. Meijer at T. U. Eindhoven, The Netherlands, he moved to the group of Paul Barbara at the University of Texas at Austin as a postdoctoral researcher, where he is currently working on the photophysical properties of single conjugated polymer molecules embedded in functioning devices.

So-Jung Park received her Ph.D. from Northwestern University in 2002 for work with Professor Chad Mirkin on DNA-linked nanoparticle networks. She is currently working on correlated electrical modulation and single-molecule optical measurements as a postdoctoral fellow in the group of Professor Paul Barbara at the University of Texas at Austin.

Young Jong Lee received a Ph.D. degree from Seoul National University in 2001 for work with Professor Seong Keun Kim on photophysics of atoms, molecules, and macromolecules. Since he joined Professor Barbara's group as a postdoctoral fellow, his work has been focused on ultrafast spectroscopy of the hydrated electron and single-molecule spectroscopy of conjugated polymers.

10.1021/ar040141w CCC: $30.25
Published on Web 06/24/2005

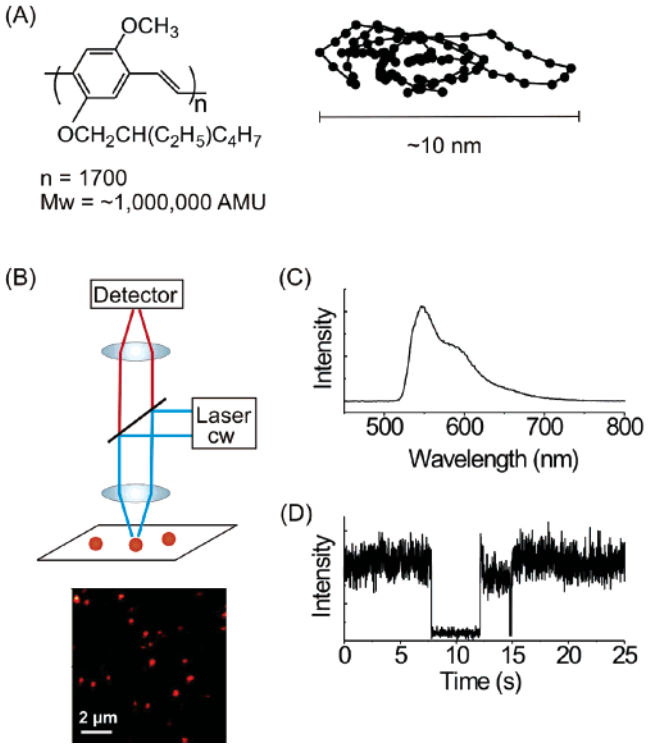

FIGURE 2. (A) Chemical structure of MEH−PPV and the conformation of isolated single polymers in a spin-coated inert polymer matrix, (B) single-molecule fluorescence apparatus, and (C) a spectrum and (D) intensity vs time trace data for a typical MEH−PPV single molecule in an inert polymer film at room temperature.

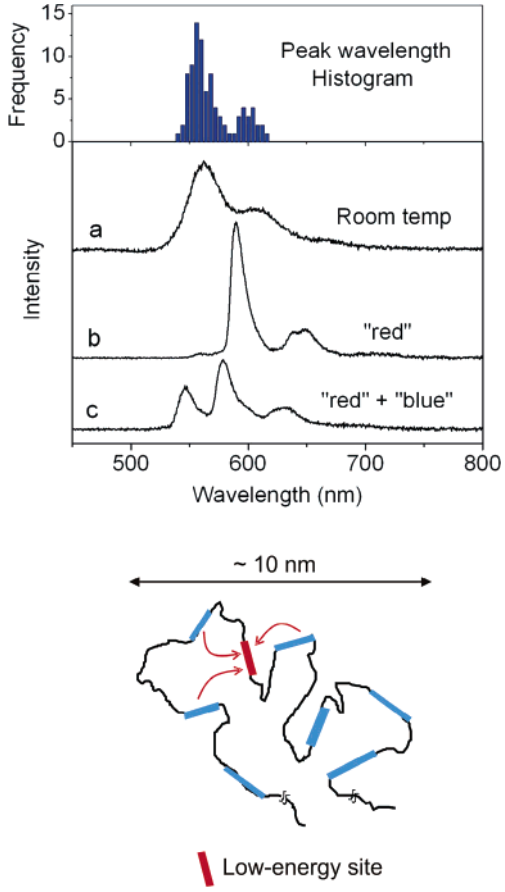

FIGURE 3. Low-temperature single-molecule spectra of MEH−PPV in an inert polymer film.

especially single-molecule spectroscopy (SMS), as described extensively in this special issue. Most of the published applications of SMS are concerned with biological problems, but SMS has also been extensively used in the investigation of highly heterogeneous semiconductor nanomaterials, including inorganic semiconductor nanocrystals,[5] and the topic of this Account, conjugated polymer single molecules.[4,6−29]

This Account reviews how SMS has added to the understanding of the structure, photophysics, photochemistry, and device physics of conjugated polymers especially for the conjugated polymer poly[2-methoxy-5-(2′-ethylhexyloxy)-1,4-phenylenevinylene] (MEH-PPV, see Figure 2A).[4,6−29] By investigating the spectroscopy of conjugated polymers, one molecule at a time in a dilute inert polymer host using a combined microscope/spectrometer (Figure 2B), researchers have been able to acquire spectral data (Figure 2C) and kinetic data (Figure 2D) for conjugated polymers that are not significantly obscured by sample heterogeneity. This has allowed for the unraveling of complex kinetic mechanisms and for the determination of distribution functions for rate constants, not just ensemble average values.

More advanced modulation SMS techniques[25,26] have opened the door to the investigation of the interaction of singlet and triplet excitons in conjugated polymers, which is relevant to the applications of these materials. SMS has also been used to study conjugated polymers incorporated in functioning organic electronic devices.[19,20,27,28] The complexity and heterogeneity of nanomaterial-based devices is a major obstacle to the effective investigation of these devices by bulk ensemble measurements, such as current−voltage (*I*−*V*) measurements and photoluminescence studies. By employment of isolated polymer chains rather than bulk materials, the diffusion of excitons and polarons is confined to a single particle and to a short separation distance, thus simplifying the investigation of many device processes. The remaining sections of this Account describe in detail recent SMS results on conjugated polymers emphasizing results from our own laboratory.

Electronic Energy Landscape of Conjugated Polymers

Light absorption and emission in conjugated polymers is due to a large number and broad distribution of quasi-localized chromophores on the polymer chains, connected by chemical and structural defects, as represented in Figure 3. For the MEH−PPV molecules in this study, there are ~200 effective chromophores, each with ~10−17 repeat units in conjugation length, in a single molecule. Absorption of photons excites different chromophores on the polymer chain (e.g., blue regions). Each isolated chain in the SMS approach is large enough (typically 10^4−10^6 amu) to be representative of the bulk in terms of spectroscopic properties and the presence of multiple chromophoric sites. Efficient electronic energy transfer funnels

the excitation to the lowest energy chromophores during the exciton lifetime (~300 ps). Thus, the fluorescence properties most often characterize those of the few low-transition-energy exciton traps in a conjugated polymer molecule despite its multichromophoric nature in light absorption.

The low-temperature SMS study by Yu and Barbara gives clear evidence for the efficient electronic energy funneling to a small number (one in many cases) of low-energy sites.[23] As shown in Figure 3, the 20 K spectra (Figure 3b,c) are much shaper than the 300 K spectra (Figure 3a) with the spectral line width (full width at half-maximum, fwhm) decreasing from ~37 nm (or ~1120 cm^{-1} in energy) at 300 K to 10 nm (~300 cm^{-1} in energy) at 20 K. The narrow line width allows us to resolve emission from different chromophores in single conjugated polymer chains. Two types of spectra were observed: single chromophoric type (Figure 3b) and multichromophoric type spectra (Figure 3c). The 0−0 and 0−1 vibronic peaks are clearly resolved in the 20 K single-chromophore-type fluorescence spectrum b in Figure 3. The observation of more than one emitting site for some of the single molecules emphasizes that multiple energy transfer channels are present in a single MEH−PPV molecule and demonstrates the power of SMS for making detailed observations on multichromophoric systems.

The histogram of low-temperature spectra shows that a significant fraction (about $^1/_3$) of the conjugated polymer chains possesses "red" sites (i.e., low-energy chromophores), Figure 3 (upper panel). The remaining molecules lack "red" sites and emit to the blue. The "red" sites are believed to be due to conjugated chain contacts, which cause a local lowering of the exciton energy due to π stacking. These data nicely demonstrate the ability of SMS to unravel the complex "distribution" of localized emitting states in conjugated polymers. It is important to note that all of the information shown in Figure 3 is completely obscured in the "bulk" ensemble spectra of these samples due to static disorder. Interestingly, in the bulk conjugated polymer (which is most relevant to the actual device application) virtually all the emission occurs from "red" sites. Apparently, the existence of "red" emission in the bulk material is due to highly efficient energy transfer to the low concentration of red sites.

Conformations of Single Conjugated Polymer Chains

Optical and electrical properties of conjugated polymers depend highly on the conformation of the polymer chains. The range of conformations adopted by conjugated polymers and other synthetic polymers has been explored by Hu et al using bead-on-a-chain simulations.[15] Distinct conformational classes are predicted, depending on the stiffness of the polymer chains and the strength of attractive interactions between segments within a chain, as shown in Figure 4A. For example, flexible polymers should adopt highly disordered conformations of either a random coil or molten globule. In contrast, stiff polymers with strong intrachain interactions, such as conjugated polymers, are expected to collapse into conformations with long-range order, in the shape of toroids or rodlike structures.

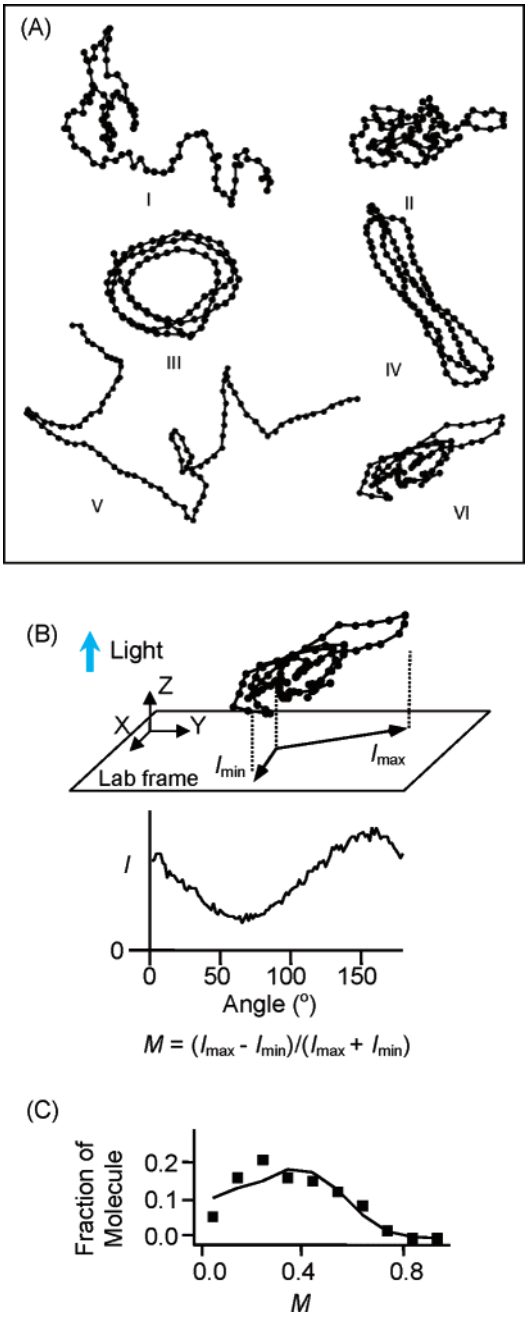

FIGURE 4. (A) Typical conformations (**I**, random coil; **II**, molten globule; **III**, toroid; **IV**, rod; **V**, defect-coil; and **VI**, defect-cylinder) of a 100-segment homopolymer generated by Monte Carlo simulations, (B) single-molecule polarization spectroscopy of MEH−PPV, and (C) the distribution of modulation depths *M* from single-molecule polarization spectroscopy (■) and from Monte Carlo simulations based on defect-cylinder conformation (—).

Single-molecule polarization spectroscopy,[15] combined with these theoretical simulations, has been used to determine conformations adopted by conjugated polymer molecules in an inert polymer matrix, Figure 4B,C. The fluorescence intensity was collected from individual MEH−PPV molecules while the direction of polarization

of the excitation light was modulated between 0° and 180°, Figure 4B. The anisotropy distribution M obtained from the measurements and bead-on-a-chain Monte Carlo simulation indicate that this prototypical stiff conjugated polymer adopts a highly ordered, collapsed conformation that is different from ideal toroid or rod structures. Indeed, it is unlikely that real conjugated polymer chains would be sufficiently free of defects to fold into the toroid or rod structures. Structure **VI** in Figure 4A is a simulated conformation for stiff chains with defects and intersegment attraction. The experimental anisotropy agrees fairly well with the simulated anisotropy distribution of this roughly cylindrical conformation, Figure 4C, demonstrating that the "tetrahedral chemical defects", where conjugated carbon−carbon links are replaced by tetrahedral links, induce the polymer chains to fold into structurally identifiable cylindrical conformations. The highly ordered, cylindrical conformations should be a critical factor in dictating the extraordinary photophysical properties of conjugated polymers, including highly efficient intramolecular energy transfer and significant local optical anisotropy in thin films.

To test the limits of the highly ordered conformation energy funneling model, Hu et al. have studied broken-conjugation MEH−PPV that contained varying amounts of single-bond defects that replace carbon−carbon double bonds in the phenylene−vinylene backbone.[18] For highly conjugated chains, singlet excitons were observed to be efficiently funneled over nanometer distances to a small number of sites. In contrast, chains with less conjugation and a high number of saturated bonds do not exhibit energy funneling due to a highly disordered conformation. Single-molecule polarization spectroscopy on these samples showed that the conformational order of a single polymer chain was observed to substantially decrease as the number of single-bond defects is increased synthetically. These results are highly consistent with the energy funneling model and further establish the special role of intramolecular order in conjugated polymer photophysics.

A different approach to the investigation of single conjugated polymer molecule conformations was taken by Lammi et al.[21] These authors used polarization SMS to investigate the conformation and orientation of conjugated polymers dissolved at low concentration in a single domain liquid crystal environment. Near-perfect orientational order of the stiff, rodlike conjugated polymers translating through a planar nematic phase was observed. This represents striking experimental evidence for the previously predicted enhanced alignment of long rod-shaped molecules in the nematic phase of a binary mixture of shorter rod-shaped molecules. Link et al extended this work to study the alignment of conjugated polymer single molecules with broken conjugation.[29] Two kinds of order parameters were considered to elucidate a meaningful structural model for our observation: one for the polymer, which is essentially an ensemble of segments, S_o ($= \langle ({}^3/_2)\cos^2 \alpha - ({}^1/_2)\rangle$, where α is the tilt angle between the major axis of the chain and the LC director), and the other for the orientation distribution of segments within the polymer chain, S_c ($= \langle ({}^3/_2)\cos^2 \beta - ({}^1/_2)\rangle$, where β is the angle between each segment and the polymer principle internal axis, that is, the direction of maximum orientation). The polarization SMS and Monte Carlo beads-on-a-chain simulations in the presence of anisotropic solvation revealed that both the orientational order (S_o) and the conformational order (S_c) decrease with increasing amounts of defects.

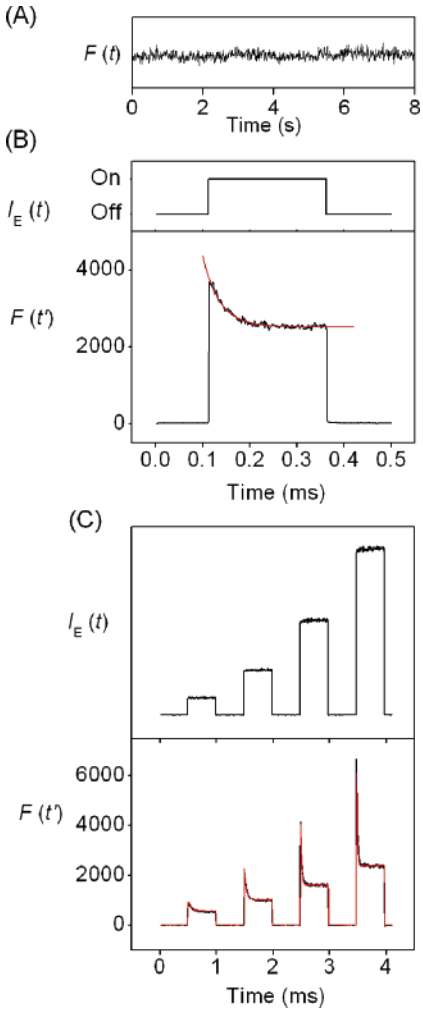

FIGURE 5. (A) Fluorescence intensity ($F(t)$) trajectory of a single MEH−PPV molecule irradiated by a repetitive sequence of excitation pulses, (B) irradiation intensity modulation sequence and synchronously time-averaged fluorescence transient ($F(t')$) of a single MEH−PPV molecule, and (C) time-averaged fluorescence transient ($F(t')$) from a single MEH−PPV molecule irradiated with different excitation intensities.

Excited Triplet States of Conjugated Polymers

While a great deal is understood about singlet excitons in conjugated polymers, much less is known about triplet excitons mainly because triplets are nonemissive or "dark" and as a result cannot usually be directly observed by emission spectroscopy. Gesquiere et al. have introduced a high signal-to-noise technique for studying triplet dynamics in multichromophoric molecules, namely, single-molecule excitation intensity modulation spectroscopy, Figure 5B.[26] In this approach, the fluorescence intensity,

$F(t)$, of a single conjugated polymer molecule is recorded while the molecule is irradiated with many repetitive cycles of a sequence of submillisecond time scale excitation pulses. The signal-to-noise ratio in an emission transient, $F(t)$, is too small to allow for the real-time intensity observation $F(t)$ of "triplet blinking" (Figure 5A). Therefore, $F(t)$ is averaged over many cycles to yield time ensemble intensity, $F(t')$, versus t' curves, where t' refers to time within the cycle, Figure 5B. Thus, $F(t')$ data can be analyzed to determine the kinetics of triplet formation and decay as a function of the time history of the irradiation.

Kinetic modeling demonstrates that the observed $F(t')$ behavior is a consequence of triplet−triplet annihilation and singlet quenching by triplets in the conjugated polymers. During the excitation off period, triplet excitons decay through reverse intersystem crossing ($T_1 \rightarrow S_0$), and the initial emission intensity $F(t')$ immediately after the excitation pulse is on reflects the emission of an essentially triplet-free molecule. As time progresses, multiple excitations ($S_0 \rightarrow S_1$) occur causing a build-up of triplet excitons by forward intersystem crossing ($S_1 \rightarrow T_1$). The fluorescence intensity decreases as the triplet population increases due primarily to singlet quenching by triplets ($S_1 + T_1 \rightarrow S_0 + T_1$) in the multichromophoric conjugated polymer molecule. The triplet population eventually reaches a steady-state population due to triplet−triplet annihilation ($T_1 + T_1 \rightarrow S_1 + S_0$). This corresponds to the plateau in the $F(t')$ data during the period when the excitation is on.

The observed $F(t')$ data are highly consistent with predictions from the recently developed kinetic population state model for multichromophoric conjugated polymers.[25] In this model, the excited states of conjugated polymer single molecules are described in terms of localized excitons, that is, $(N_S,N_T) \rightarrow (N_S',N_T')$, where N_S, N_T, N_S', and N_T' are the number of singlet and triplet excitons in the entire chain before and after the specific photophysical process, respectively. The conjugated polymer is predicted to spend most of the time in either (0,0) or (0,1) states, and the population kinetic scheme can be approximated to the following two-state model:

$$(0,0) \underset{k_B}{\overset{k_F}{\rightleftharpoons}} (0,1) \qquad (1)$$

with forward and backward first-order rate constants, k_F and k_B, that are given by

$$k_F = k_{exc}k_{isc}\tau_{fl} \qquad (2)$$

$$k_B = k'_{isc} + k_{exc}k_{isc}\tau'_{fl} \qquad (3)$$

where k'_{isc} is the reverse ISC rate, k_{isc} is the ISC rate, τ_{fl} is the fluorescence lifetime of the (1,0) state, and τ'_{fl} is the fluorescence lifetime of the (1,1) state. The second term of eq 3 represents the contribution from the triplet−triplet annihilation. The relaxation of the (1,1) state involves an additional relaxation process, namely, singlet quenching by a triplet exciton, and thus τ'_{fl} is expected to be shorter than τ_{fl}. The effect of singlet quenching by triplets is quantified by the rate constant for singlet quenching by a triplet in a single molecule, k_{QST} ($= 1/\tau'_{fl} - 1/\tau_{fl}$).

Table 1. The Rate Constants for Reverse Intersystem Crossing (k'_{isc}) and Quenching of Singlets by Triplets (k_{QST}) Determined for Several MEH−PPV Molecules in an Inert Polymer Matrix

molecule	k'_{isc} (s^{-1})	k_{QST} (s^{-1})
1	5.0×10^3	2.7×10^9
2	5.0×10^3	6.4×10^{10}
3	8.0×10^3	3.0×10^{10}
4	10.0×10^3	1.3×10^{10}
5	8.0×10^3	3.0×10^{10}
6	6.0×10^3	8.0×10^{10}

Figure 5B,C shows global fits of the kinetic model[26] to experimental data at various excitation pulse intensities. A significant observation from the power dependence study is that at high power the reverse intersystem crossing rate is much smaller than the rate of triplet−triplet annihilation (i.e., $k'_{isc} \ll k_{exc}k_{isc}\tau'_{fl}$), and the latter process is dominant. The parameters extracted from the modulation data are given in Table 1. The best fit values of k_{QST} show that singlet quenching by a triplet exciton is an extremely rapid process occurring on the tens to hundreds of picoseconds time scale. This process is likely to occur via a Förster energy transfer, since the calculated Förster energy transfer rate (10^{10} s^{-1}) is close to the experimental value.

Fluorescence−Voltage/Single-Molecule Spectroscopy (*F*−*V*/SMS)

Park et al. recently introduced a new technique that allows for SMS in a device environment.[19,20] This technique, which we denote *F*−*V*/SMS, involves simultaneous single-molecule fluorescence spectroscopy while controlling oxidation/reduction of individual molecules or nanoparticles using a charge injection device. This approach is particularly useful for studying the interactions between excitons and polarons. It is achieved by recording the single-molecule fluorescence intensity as a function of device bias, which controls the population of polarons. This method also offers a unique means for characterizing the chemical nature of the photochemically induced intermediate states of conjugated polymers that are responsible for fluorescence "blinking" and "flickering". By studying the bias dependence of the SMS data during the lifetime of the fluorescence "flickering" intermediate, one can obtain information on the oxidation/reduction properties (e.g., HOMO energies) of the intermediate. An example of *F*−*V*/SMS data is presented in Figure 6, which shows the fluorescence intensity of a single isolated MEH−PPV molecule as a function of the bias voltage *V*. The *F*−*V*

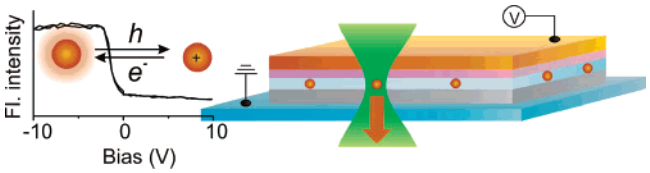

FIGURE 6. Configuration of a typical *F*−*V*/SMS setup and *F*−*V*/SMS data.

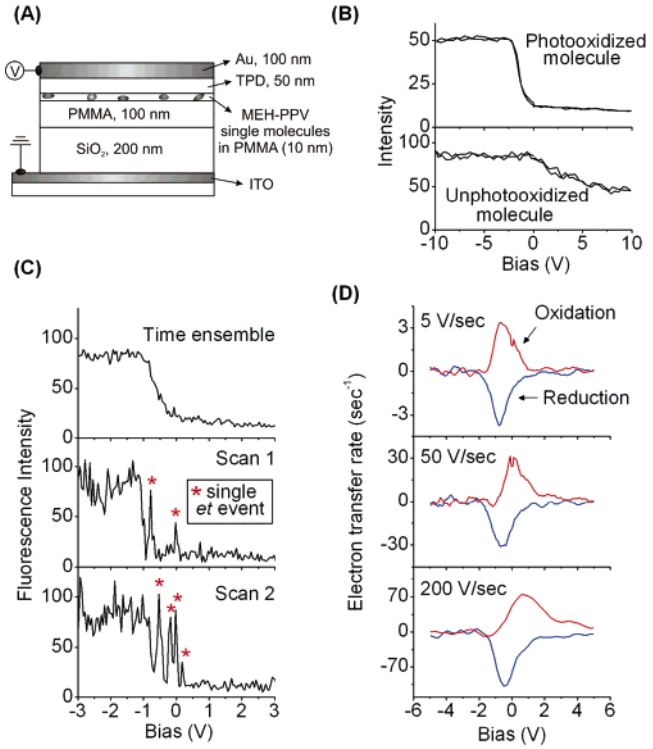

FIGURE 7. (A) A diagram of a capacitor-like hole injection device, (B) two typical bias-dependent modulation behaviors, *F*−*V* curves collected from (top) a photooxidized molecule showing a discrete fluorescence quenching by a hole injection and (bottom) an unphotooxidized molecule showing a gradual fluorescence quenching at positive bias by TPD holes, (C) *F*−*V*/SMS time ensemble (top) and individual scans (middle and bottom) of a photooxidized MEH−PPV molecule, and (D) electron-transfer rate vs bias curves collected at different scan rates.

curve reveals that a single positive charge (hole) injected from the device induces a significant quenching of the MEH−PPV fluorescence. This technique is analogous in several ways to current vs voltage (*I*−*V*) measurements for devices and electrochemical cells. For example, *F*−*V*/SMS data at different scan rates can be analyzed to study both energetics and kinetics of charge transfer (oxidation/reduction) processes of the isolated single molecules. *F*−*V*/SMS data of this type can be used to sort-out the complex mechanism of charge transport, interface charging, and actual electron transfer on a molecule-by-molecule and location-by-location basis in a device.

The capacitor-like hole injection device employed for this study is described in Figure 7A. In the device configuration, holes are injected from the gold electrode to the hole transport layer of *N*,*N*′-bis(3-methylphenyl)-*N*,*N*′-diphenylbenzidine (TPD) at positive bias. In typical experiments, fluorescence intensity vs time traces of isolated single MEH−PPV molecules are collected while a triangular wave bias voltage sequence is repeatedly applied to the device, and then the SMS data are averaged over many cycles of the bias and replotted in the form of an *F*−*V* curve. At zero bias, fluorescence vs time traces of the molecules in a device show typical fluorescence intensity fluctuations observed from MEH−PPV single molecules in an inert polymer matrix (e.g., Figure 2D). The fluorescence flickering in single conjugated polymers has been attributed to efficient energy funneling to a photooxidation-induced quencher site.

Two distinct bias-dependent behaviors were observed depending on the chemical state of the MEH−PPV molecules. For unphotooxidized MEH−PPV molecules, fluorescence quenching was observed at positive bias (Figure 7B, bottom). The gradual dependence of the quenching efficiency on bias for the unphotooxidized molecules is consistent with the singlet exciton quenching by hole polarons present in the hole transport layer (TPD). Significantly, while molecules are at the fluorescence flickering intermediate state (photooxidized), an extraordinary repairing of photobleaching was observed for negative bias, Figure 7B. The discrete sigmoidal behavior of photooxidized molecule near −1.5 V is indicative of a reversible single electron transfer event. The spikes of fluorescence intensity at the transition region in individual scans further demonstrate that the electron transfer process involves a single electron transfer per molecule (Figure 7C). The intensity fluctuations at the transition region reflect the stochastic nature of electron transfer, not photon shot noise, which is much smaller. Importantly, this behavior indicates that the long-lived quencher sites can be reversibly oxidized and reduced, and it suggests that the photobleached form of the polymer is a charged species (i.e., MEH−PPV^+/anion complex). Such a complex could be formed by photoinduced electron transfer between MEH−PPV and oxygen, forming MEH−PPV^+/O_2^-, which could further react with water, a common impurity, resulting in a more stable anion, OH^-. The reversible oxidation/reneutralization and extraordinary bias-induced repair process excludes typical singlet oxygen oxidation products such as dioxetanes and endoperoxides, since these latter species would not be reduced by charge carriers. Photoinduced electron transfer is indeed consistent with well-known, but poorly understood, persistent photoconductivity of MEH−PPV thin films upon exposure to air.

Charge injection dynamics of single molecules in the device were diverse, and hysteresis was often observed in the oxidation/reduction potential. To study the charge injection dynamics of this system, *F*−*V* curves were acquired at different scan rates. For time averaged *F*−*V* data, the fluorescence intensity is determined by the time-averaged probability ($P(t)$) of occupying the oxidized form, and the number of oxidation events per unit time per molecule (R) is defined by dP/dt. Using this definition, we converted the *F*−*V* curves collected from the same photooxidized molecule to *R* vs *V* curves, Figure 7D. The resulting positive and negative peaks in *R* vs *V* curves represent oxidation (from −5 to 5 V) and reduction (from 5 to −5 V) scans, respectively. These data clearly show that at faster scan rates, the charge injection is too slow to keep up with time varying voltage. At a slower scan rate (5 V/sec), the oxidation and reduction peaks are located at nearly the same potential. Extensive *F*−*V*/SMS measurements on a large number of different molecules and devices show that kinetics vary greatly from one

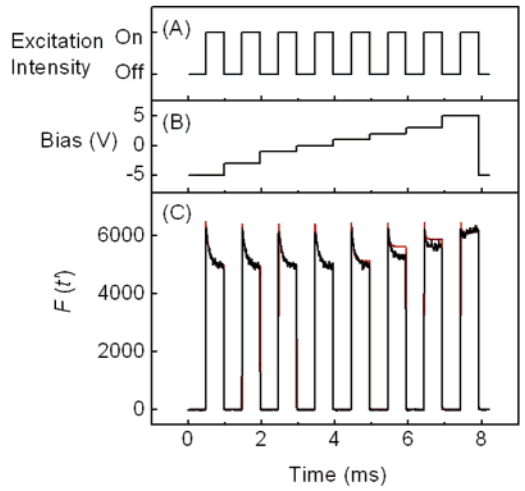

FIGURE 8. Fluorescence intensity collected for single MEH−PPV molecules while simultaneously modulating the device bias and the irradiation intensity.

molecule to another in the sample due to the inhomogeneity of the device interface.

Fluorescence−Voltage Time-Resolved SMS

Recently, there has been a growing appreciation that dynamical processes involving the interaction of triplet excitons with polarons can play an important role in the performance of polymer OLED and related organic electronic devices. Gesquiere et al. have used a technique, fluorescence−voltage time-resolved single-molecule spectroscopy (*F*−*V*-TR-SMS), to obtain quantitative information on the mechanisms and rates of hole polaron-induced quenching of triplet and singlet excitons.[27] This approach combines the two above-described techniques (single-molecule excitation intensity modulation spectroscopy and *F*−*V*/SMS) and measures the fluorescence intensity of a single molecule embedded in an electronic device while simultaneously modulating the irradiation intensity (Figure 8A) and the bias on the device (Figure 8B).

Figure 8 shows *F*−*V*-TR-SMS data obtained for a single MEH−PPV molecule in contact with the hole transport layer (TPD) of a hole-injection, capacitor-like device structure described in Figure 7A. The observed *F*−*V*-TR-SMS data varied for different MEH−PPV molecules but was constant over time for any individual molecule. Negative-bias device environment results are similar to the inert polymer host measurements, consistent with the expectation that at negative bias the capacitor device is depleted of polarons. For biases above the threshold for hole injection (~1 V), the *F*−*V*-TR-SMS data show shorter decay times and a smaller difference between the fluorescence intensity right after the excitation pulse is on and the fluorescence intensity at the "plateau". This observation is highly consistent with triplet quenching by TPD hole polarons, p^+,

$$p^+ + T_1 \xrightarrow{k_{QT}} p^+ + S_0 \qquad (4)$$

Table 2. Best-Fit Kinetic Parameters for Different MEH−PPV Molecules in a Capacitor Device Environment[a]

molecule	k'_{isc} (s^{-1})	k_{QST} (s^{-1})	k_{QT} ($mol^{-1}\ s^{-1}$)	k_{QS} ($mol^{-1}\ s^{-1}$)	E_{QT} (%)[d]	E_{QS} (%)[e]
1	6.0×10^3	7.0×10^9	1.1×10^7	$[3.0 \times 10^6]$[c]	100	0
2	6.0×10^3	5.3×10^9	1.1×10^9	1.6×10^{11}	100	24
3	4.0×10^3	4.3×10^9	1.1×10^9	1.1×10^{12}	100	70
4	6.0×10^3	3.8×10^9	*b*	*b*	0	0

[a] In the fitting procedures, a quantum yield of intersystem crossing of 1.25% was used for MEH−PPV. [b] No polarons are interacting with the molecule, so no rate constant is reported. [c] This value is an upper limit for k_{QS}. [d] Defined as $(F(\text{plateau})_{V=5V} - F(\text{plateau})_{V<V_0})/(F(\text{initial}) - F(\text{plateau}))_{V<V_0}$ in the case of triplet quenching only. When singlet quenching is observed, the triplet quenching efficiency is 100%. [e] Defined as $(F(\text{initial})_{V<V_0} - F(\text{initial})_{V=5V})/F(\text{initial})_{V<V_0}$.

which presumably occurs by a charge-transfer mechanism, perhaps involving the intermediacy of a MEH−PPV hole polaron. Singlet exciton quenching by TPD hole polarons (eq 5) was also observed in these devices.

$$p^+ + S_1 \xrightarrow{k_{QS}} p^+ + S_0 \qquad (5)$$

This mechanism may involve spin-allowed energy transfer or charge transfer.

The data are well-fit by our previously described kinetic model[25−27] (parameters in Table 2) with the exception of the slowly varying intensity changes during each pulse region at positive bias ($V > V_0$). The slowly varying regions are assigned to a noninstantaneous response of the local quasi-Fermi-potential in the device due to the filling of deep hole traps in the hole-transporting layer of the device.

A significant result from this study is the observation that triplet excitons are much more efficiently quenched than singlet excitons. This is summarized in Table 2, where the efficiency of triplet and singlet quenching by hole polarons, E_{QT} and E_{QS}, is shown for $V(t) = 5$ V for various molecules. More efficient quenching of triplets occurs despite the fact that the triplet quenching rate constant, k_{QT}, is in fact several orders of magnitude slower than that for singlets (k_{QS}). The more efficient quenching of triplets is probably due to a factor of 10^6 greater lifetime for the triplet exciton compared to the singlet exciton. This result suggests that singlet and triplet quenching by hole polarons occurs by different mechanisms. The singlet quenching process can in principle occur by a spin-allowed energy-transfer process, analogous to that described above for the quenching of singlet excitons by triplet excitons. The quenching of triplet excitons by polarons is a spin-forbidden process, and a slower charge-transfer mechanism is probably operating for triplets.

Probing a Molecular Interface in a Functioning Organic Diode

Lee et al. have used *F*−*V*/SMS to study a hole-injection/hole-transport interface within a functioning organic diode (Figure 9).[28] MEH−PPV single molecules were dispersed at the interface between the hole-injection and hole-transport layers to create and probe singlet and

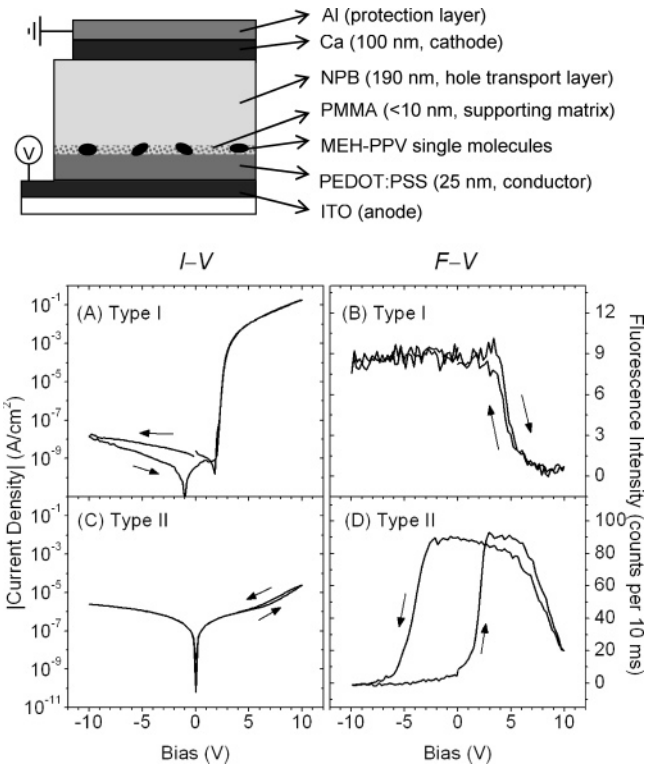

FIGURE 9. *F*−*V*/SMS of MEH−PPV imbedded in a functioning diode.

triplet excitons at the heterojunction. Figure 9 shows representative *F*−*V* curves from single molecules along with *I*−*V* data of the diode. Efficient exciton quenching is observed at high forward bias due to a build-up of interfacial polaron density, Figure 9A,B. Additionally, for some diodes, an unexpected quenching process was also observed at reverse bias, which is ascribed to hole charging of the interface due to the leakage current, Figure 9C,D.

Conclusions and Future Directions

Several new SMS techniques have been developed and applied to study molecular structure, photophysics, and device physics of conjugated polymer single molecules. These materials have been investigated in environments ranging from inert polymer films to single domain liquid crystal hosts and functioning electronic devices. The results offer new insights on how the morphology of conjugated polymers can impact the photodynamics and spectroscopy of these materials. In addition, time-resolved SMS measurements have unraveled complex interactions among singlet excitons, triplet excitons, and hole polarons in conjugated polymer based electronic devices.

In the future, we plan to broadly apply the SMS techniques described herein to study conjugated polymers and organic/inorganic hybrid materials in promising device architectures. These experiments will offer in principle a new level of understanding of how molecular-level processes impact the performance of electronic devices based on these materials.

Financial support by the National Science Foundation, the Welch Foundation, and the Keck Foundation is gratefully acknowledged. The authors also thank our numerous co-workers that are listed in many of the references of this paper.

References

(1) Wang, H. L.; MacDiarmid, A. G.; Wang, Y. Z.; Gebler, D. D.; Epstein, A. J. Application of polyaniline (emeraldine base, EB) in polymer light-emitting devices. *Synth. Met.* **1996**, *78*, 33−37.
(2) Hide, F.; Diazgarcia, M. A.; Schwartz, B. J.; Heeger, A. J. New developments in the photonic applications of conjugated polymers. *Acc. Chem. Res.* **1997**, *30*, 430−436.
(3) Friend, R. H.; Gymer, R. W.; Holmes, A. B.; Burroughes, J. H.; Marks, R. N.; Taliani, C.; Bradley, D. D. C.; Dos Santos, D. A.; Bredas, J. L.; Logdlund, M.; Salaneck, W. R. Electroluminescence in conjugated polymers. *Nature* **1999**, *397*, 121−128.
(4) Vanden Bout, D. A.; Kerimo, J.; Higgins, D. A.; Barbara, P. F. Near-field optical studies of thin-film mesostructured organic materials. *Acc. Chem. Res.* **1997**, *30*, 204−212.
(5) Nirmal, M.; Dabbousi, B. O.; Bawendi, M. G.; Macklin, J. J.; Trautman, J. K.; Harris, T. D.; Brus, L. E. Fluorescence intermittency in single cadmium selenide nanocrystals. *Nature* **1996**, *383*, 802−804.
(6) Huser, T.; Yan, M.; Rothberg, L. J. Single chain spectroscopy of conformational dependence of conjugated polymer photophysics. *Proc. Natl. Acad. Sci. U.S.A.* **2000**, *97*, 11187−11191.
(7) Sartori, S. S.; De Feyter, S.; Hofkens, J.; Van der Auweraer, M.; De Schryver, F.; Brunner, K.; Hofstraat, J. W. Host matrix dependence on the photophysical properties of individual conjugated polymer chains. *Macromolecules* **2003**, *36*, 500−507.
(8) Mehta, A.; Kumar, P.; Dadmun, M. D.; Zheng, J.; Dickson, R. M.; Thundat, T.; Sumpter, B. G.; Barnes, M. D. Oriented nanostructures from single molecules of a semiconducting polymer: polarization evidence for highly aligned intramolecular geometries. *Nano Lett.* **2003**, *3*, 603−607.
(9) Ronne, C.; Tragardh, J.; Hessman, D.; Sundstrom, V. Temperature effect on single chain MEH−PPV spectra. *Chem. Phys. Lett.* **2004**, *388*, 40−45.
(10) Wang, C. F.; White, J. D.; Lim, T. L.; Hsu, J. H.; Yang, S. C.; Fann, W. S.; Peng, K. Y.; Chen, S. A. Illumination of exciton migration in rodlike luminescent conjugated polymers by single-molecule spectroscopy. *Phys. Rev. B* **2003**, *67*, No. 035202.
(11) Schindler, F.; Lupton, J. M.; Feldmann, J.; Scherf, U. A universal picture of chromophores in pi-conjugated polymers derived from single-molecule spectroscopy. *Proc. Natl. Acad. Sci. U.S.A.* **2004**, *101*, 14695−14700.
(12) Vandenbout, D. A.; Yip, W. T.; Hu, D. H.; Fu, D. K.; Swager, T. M.; Barbara, P. F. Discrete intensity jumps and intramolecular electronic energy transfer in the spectroscopy of single conjugated polymer molecules. *Science* **1997**, *277*, 1074−1077.
(13) Yip, W. T.; Hu, D. H.; Yu, J.; Vanden Bout, D. A.; Barbara, P. F. Classifying the photophysical dynamics of single- and multiple-chromophoric molecules by single molecule spectroscopy. *J. Phys. Chem. A* **1998**, *102*, 7564−7575.
(14) Hu, D. H.; Yu, J.; Barbara, P. F. Single-molecule spectroscopy of the conjugated polymer MEH−PPV. *J. Am. Chem. Soc.* **1999**, *121*, 6936−6937.
(15) Hu, D. H.; Yu, J.; Wong, K.; Bagchi, B.; Rossky, P. J.; Barbara, P. F. Collapse of stiff conjugated polymers with chemical defects into ordered, cylindrical conformations. *Nature* **2000**, *405*, 1030−1033.
(16) Yu, J.; Hu, D. H.; Barbara, P. F. Unmasking electronic energy transfer of conjugated polymers by suppression of O-2 quenching. *Science* **2000**, *289*, 1327−1330.
(17) Wong, K. F.; Skaf, M. S.; Yang, C. Y.; Rossky, P. J.; Bagchi, B.; Hu, D. H.; Yu, J.; Barbara, P. F. Structural and electronic characterization of chemical and conformational defects in conjugated polymers. *J. Phys. Chem. B* **2001**, *105*, 6103−6107.
(18) Hu, D. H.; Yu, J.; Padmanaban, G.; Ramakrishnan, S.; Barbara, P. F. Spatial confinement of exciton transfer and the role of conformational order in organic nanoparticles. *Nano Lett.* **2002**, *2*, 1121−1124.
(19) Park, S. J.; Gesquiere, A. J.; Yu, J.; Barbara, P. F. Charge injection and photooxidation of single conjugated polymer molecules. *J. Am. Chem. Soc.* **2004**, *126*, 4116−4117.
(20) Gesquiere, A. J.; Park, S. J.; Barbara, P. F. F−V/SMS: A new technique for studying the structure and dynamics of single

molecules and nanoparticles. *J. Phys. Chem. B* **2004**, *108*, 10301−10308.
(21) Lammi, R. K.; Fritz, K. P.; Scholes, G. D.; Barbara, P. F. Ordering of single conjugated polymers in a nematic liquid crystal host. *J. Phys. Chem. B* **2004**, *108*, 4593−4596.
(22) Yu, J.; Song, N. W.; McNeill, J. D.; Barbara, P. F. Efficient exciton quenching by hole polarons in the conjugated polymer MEH−PPV. *Isr. J. Chem.* **2004**, *44*, 127−132.
(23) Yu, Z. H.; Barbara, P. F. Low-temperature single-molecule spectroscopy of MEH−PPV conjugated polymer molecules. *J. Phys. Chem. B* **2004**, *108*, 11321−11326.
(24) Lammi, R. K.; Barbara, P. F. Influence of chain length on exciton migration to low-energy sites in single fluorene copolymers. *Photochem. Photobiol. Sci.* **2005**, *4*, 95−99.
(25) Yu, J.; Lammi, R. K.; Gesquiere, A. J.; Barbara, P. F. Singlet−triplet and triplet−triplet interactions in conjugated polymer single molecules. *J. Phys. Chem. B* **2005**, *109*, 10025.
(26) Gesquiere, A. J.; Lee, Y. J.; Yu, J.; Barbara, P. F. Single molecule modulation spectroscopy of conjugated polymers. *J. Phys. Chem. B*, published online June 2, 2005, http://dx.doi.org/10.1021/jp0507851.
(27) Gesquiere, A. J.; Park, S.-J.; Barbara, P. F. Hole polaron induced quenching of triplet and singlet excitons in conjugated polymers. *J. Am. Chem. Soc.*, published online June 14, 2005, http://dx.doi.org/10.1021/ja051271i.
(28) Lee, Y. J.; Park, S.-J.; Gesquiere, A. J.; Barbara, P. F. Probing a molecular interface in a functioning organic diode. *Appl. Phys. Lett.*, in press.
(29) Link, S.; Hu, D.; Chang, W. S.; Lammi, R. K.; Scholes, G. D.; Barbara, P. F. Nematic solvation of "broken" conjugated polymers. Submitted for publication, 2005.

AR040141W